

Toughening mechanisms of nanoparticle-modified epoxy polymers

R.D. Mohammed ^a, B.B. Johnsen ^b, A.J. Kinloch ^c, A.C. Taylor ^c, S. Sprenger ^d

^a C-IDEAS, The University of Trinidad and Tobago, O'Meara Campus, Arima, Trinidad and Tobago

^b Norwegian Defence Research Establishment, Postboks 25, 2027 Kjeller, Norway

^c Department of Mechanical Engineering, Imperial College London, South Kensington Campus, London SW7 2AZ, UK

^d Nanoresins AG, Charlottenburger Strasse 9, 21502 Geesthacht, Germany

ABSTRACT

An epoxy resin, cured with an anhydride, has been modified by the addition of silica nanoparticles. The particles were introduced via a sole gel technique which gave a very well-dispersed phase of nanosilica particles of about 20 nm in diameter. AFM and TEM showed that the nanoparticles were well-dispersed in the epoxy matrix. T_g was unchanged by the addition of the nanoparticles, but both the modulus and toughness increased. The fracture energy increased from 100J/m for the unmodified epoxy to 460J/m for the epoxy with 13 vol% of nanosilica. The fracture surfaces were inspected using SEM and AFM, and the results were compared to various toughening mechanisms proposed in the literature. The microscopy showed evidence of debonding of the nanoparticles and subsequent plastic void growth. A theoretical model of plastic void growth was used to confirm that this mechanism was indeed most likely to be responsible for the increased toughness that was observed due to the presence of the nanoparticles.

Keywords: epoxy, nanoparticles, fracture

1 INTRODUCTION

Epoxy polymers are widely used for the matrices of fibre reinforced composite materials and as adhesives. When cured, epoxies are amorphous and highly-crosslinked (i.e. thermosetting) polymers. This microstructure results in many useful properties for structural engineering applications, such as a high modulus and failure strength, low creep, and good performance at elevated temperatures.

However, the structure of such thermosetting polymers also leads to a highly undesirable property in that they are relatively brittle materials, with a poor resistance to crack initiation and growth. Nevertheless, it has been well established for many years that the incorporation of a second microphase of a dispersed rubber, e.g. [1], or a thermoplastic polymer, e.g. [2], into the epoxy polymer can increase their toughness. Here the rubber or thermoplastic particles are typically about 1–5 μ m in diameter with a volume fraction of about 5–20%. However, the presence of the rubbery phase typically increases the viscosity of the epoxy monomer mixture and reduces the modulus of the cured epoxy polymer.

Hence rigid, inorganic particles have also been used, as these can increase the toughness without affecting the glass transition temperature of the epoxy polymer. Here glass beads or ceramic (e.g. silica or alumina) particles with a

diameter of between 4 and 100 μ m are typically used, e.g. [3]. However, these relatively large particles also significantly increase the viscosity of the resin, reducing the ease of processing. In addition, due to the size of these particles they are unsuitable for use with infusion processes for the production of fibre composites as they are strained out by the small gaps between the fibres.

More recently, a new technology has emerged which holds promise for increasing the mechanical performance of such thermosetting polymers. This is via the addition of a nanophase structure in the polymer, where the nanophase consists of small rigid particles of silica [5]. Such nanoparticle modified epoxies have been shown to not only increase further the toughness of the epoxy polymer but also, due to the very small size of the silica particles, not to lead to a significant increase in the viscosity of the epoxy monomer.

The aims of the present work were to investigate the fracture toughness of epoxy polymer modified with silica nanoparticles, and to establish the structure/property relationships. The toughening mechanisms which may be operating will be reviewed, and the mechanism most likely to be responsible will be identified.

2 MATERIALS

The materials were based upon a one-component hot-cured epoxy formulation. The epoxy resin was a standard diglycidyl ether of bis-phenol A (DGEBA) with an epoxy equivalent weight (EEW) of 185 g/mol, 'Bakelite EPR 164' supplied by Hexion Speciality Chemicals, Duisburg, Germany. The silica (SiO₂) nanoparticles were supplied as a colloidal silica sol in the resin matrix, 'Nanopox F400', by Nanoresins, Geesthacht, Germany. The particles are synthesised from aqueous sodium silicate solution [5]. They then undergo a process of surface modification with organosilane and matrix exchange, to produce a masterbatch of 40 wt% (26 vol%) silica in the epoxy resin. The nanosilica particles had a mean particle size of about 20 nm, with a narrow range of particle-size distribution; laser light scattering shows that almost all particles are between 5 and 35 nm in diameter. The particle size and excellent dispersion of these silica particles remain unchanged during any further mixing and/or blending operations. Further, despite the relatively high silica content of 26 vol%, the nanofilled epoxy resin still has a comparatively low viscosity due to the agglomerate-free colloidal dispersion of the nanoparticles in the resin. The

small diameter and good dispersion of the nanoparticles of silica have been previously reported and shown [4]. The curing agent was an accelerated methylhexahydrophthalic acid anhydride, namely 'Albidur HE 600' supplied by Nanoresins, Geesthacht, Germany.

Bulk sheets of unmodified epoxy and nanosilica-modified epoxy polymers were produced to determine the properties of the polymers. Firstly, the simple DGEBA resin was mixed together with given amounts of the nanosilica-containing epoxy resin. The value of the EEW of the blend was then measured via titration. Secondly, the stoichiometric amount of the curing agent was added to the mixture, which was poured into release-coated moulds and pre-cured for 1h at 90°C, followed by a cure of 2h at 160°C.

The densities of the plates were measured. An epoxy density of 1100 kg/m³ and a silica density of 1800 kg/m³ were calculated. The volume fraction of silica was calculated from the known weight fractions using the measured densities.

3 EXPERIMENTAL

The glass transition temperature, T_g , of the various polymers was measured using differential scanning calorimetry. The sample was heated to 175°C at a rate of 10°C/min, and then cooled to 0°C. The sample was then heated again to 175°C, and the results quoted are from this second heating run.

Tensile dumbbell specimens were tested at a displacement rate of 1 mm/min and a test temperature of 21 °C, according to the ISO standard test method [6,7]. The strain in the gauge length was measured using a clip-on extensometer, and the Young's modulus, E , was calculated.

The single-edge notch bend (SENB) tests were used to determine the fracture toughness according to the relevant ISO standard [8], using a displacement rate of 1 mm/min and a test temperature of 21°C. Four replicate specimens were tested for each blend composition. The machined notch was sharpened by drawing a razor blade across the notch tip before testing. All the specimens failed by unstable crack growth, and hence only a single initiation value of the fracture toughness was obtained from each specimen.

Thin sections, approximately 60-80 nm thick, of the blends were cryo-microtomed (at -50°C) for subsequent examination using transmission electron microscopy (TEM). For atomic force microscopy (AFM) studies, a smooth surface was first prepared by cutting samples on a cryo-ultramicrotome at temperatures down to -100°C. The AFM scans were performed in tapping mode using silicon probes, and both height and phase images were recorded.

4 RESULTS

4.1 Thermo-mechanical Results

The tensile and fracture results for various nanosilica contents are given in Table 1.

Table 1
Glass transition temperatures, modulus and fracture properties of the anhydride-cured epoxy polymer containing nanosilica particles

Nanosilica content (wt%)	Nanosilica content (vol%)	T_g (°C) DSC	T_g (°C) DMTA	E (GPa)	K_{Ic} (MN m ^{-3/2})	G_{Ic} (J/m ²)
0	0	143	153	2.96	0.59	103
4.1	2.5	137	152	3.20	1.03	291
7.8	4.9	136	154	3.42	1.17	352
11.1	7.1	141	151	3.57	1.18	343
14.8	9.6	138	152	3.60	1.29	406
20.2	13.4	138	150	3.85	1.42	461

4.2 Fracture Surfaces

SEM micrographs of the fracture surfaces of selected epoxies are shown in Figure 1. Crack growth occurs from left to right. The fracture surface of the unmodified epoxy polymer is shown in Fig. 1a, where the direction of crack propagation is from left to right. The fracture surface is relatively smooth and glassy, which is typical of a brittle thermosetting polymer [10], and shows that no large-scale plastic deformation has occurred during fracture. These observations agree well with the low measured toughness of the material, where $K_{Ic} = 0.59 \text{ MN m}^{-3/2}$. In addition, there are apparent steps and changes of the level of the crack which can be observed in Fig. 1a. These features are feather markings, which are caused by the crack forking due to the excess of energy associated with the relatively fast crack growth. This repeated forking and the multi-planar nature of the surface are ways of absorbing this excess energy in a very brittle material [11]. The fracture surface of the nanosilica-modified materials showed similar features to those of the unmodified epoxy polymer, as shown in Fig. 1b and c. Crack forking and feather markings are observed, and the fracture surfaces have a brittle appearance. However, the addition of nanosilica did not give an apparent increase in the roughness observed by scanning electron microscopy, unlike for micrometre-sized particles, e.g. [9].

4.3 Toughening micromechanisms

The results were compared to various toughening mechanisms proposed in the literature, and most explanations were discounted, including crack pinning, immobilized polymer and crack deflection [13].

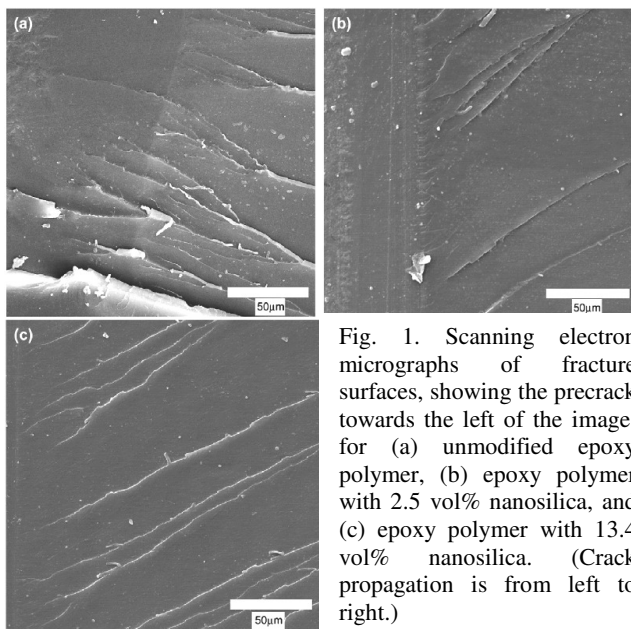


Fig. 1. Scanning electron micrographs of fracture surfaces, showing the precrack towards the left of the image, for (a) unmodified epoxy polymer, (b) epoxy polymer with 2.5 vol% nanosilica, and (c) epoxy polymer with 13.4 vol% nanosilica. (Crack propagation is from left to right.)

4.3.1 Plastic Void Growth

The toughening mechanisms associated with micrometer-sized particles have frequently been shown to be due to debonding of the particles followed by plastic void growth. Indeed, Kinloch and Taylor [10] have also demonstrated that the voids around particles closed-up when the epoxy polymer was heated above its T_g and allowed to relax. The debonding process is generally considered to absorb little energy compared to the plastic deformation of the matrix. However, debonding is essential because this reduces the constraint at the crack tip and hence allows the matrix to deform plastically via a void growth mechanism.

High resolution scanning electron microscopy (FEG-SEM) of a fracture surface of the polymer containing 9.6 vol% nanosilica, see Fig. 2, showed the presence of voids around several of the nanoparticles. This shows that plastic void growth of the epoxy matrix, initiated by debonding of the nanoparticles, has occurred. The diameter of these voids is typically 30 nm. These voids were also observed in the fracture surfaces of samples with different contents of nanosilica. Although the samples are coated to prevent charging in the electron microscope, the voids are not an artefact of the coating as they could not be observed on a coated fracture surface of the pure epoxy polymer, see Fig. 3. Also, the nanosilica modified samples appeared similar whether they were coated with platinum or gold.

In addition, similar voids were observed by AFM of uncoated fracture surfaces, see Fig. 4. However, the apparent diameter of the nanoparticle in the void highlighted in Fig. 4 is 30 nm, as shown in the graph in Fig. 4, whereas transmission electron microscopy has shown that the mean particle size is actually around 20 nm. This discrepancy is due to the tip-broadening effect when the AFM is used to identify such small features. As the tip

radius of the AFM probe is about 10 nm, this makes features that are protruding out of a surface appear larger than their true size in the micrographs. The void diameter in this case is about 70 nm, and it would appear that AFM can only be reliably used to detect the largest voids.

Voids with no nanoparticles were also observed with FEGSEM. Here the particles associated with these voids will be situated in the opposite fracture surface, or have fallen out of the surface completely during fracture, as is commonly observed with micrometre-sized particles [10]. (It should be noted that the diameters of most of these holes are less than those discussed above, as the matrix is unlikely to fail across the widest point of the void. Further, the coating, which is 5 nm thick, will partially fill the voids, and hence the observed size may be smaller than the true (uncoated) diameter.)

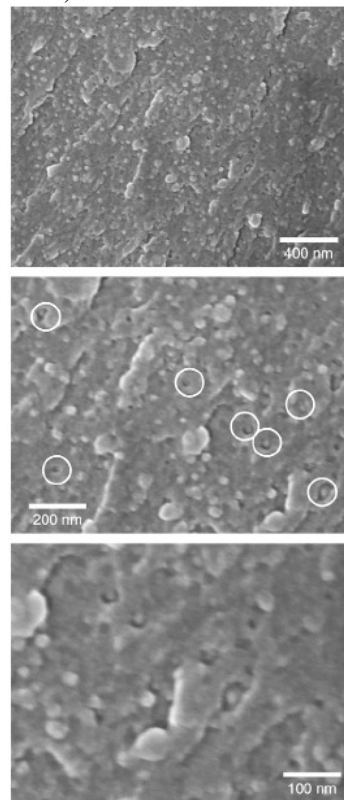


Fig. 2. Scanning electron micrographs (FEG-SEM) of the fracture surface of the epoxy polymer containing 9.6 vol% nanosilica. (Voids with nanoparticles are circled in the central image.)

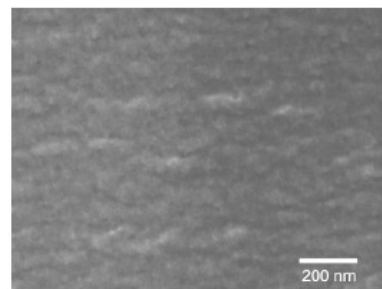


Fig. 3. Scanning electron micrograph (FEG-SEM) of the fracture surface of the unmodified epoxy polymer.

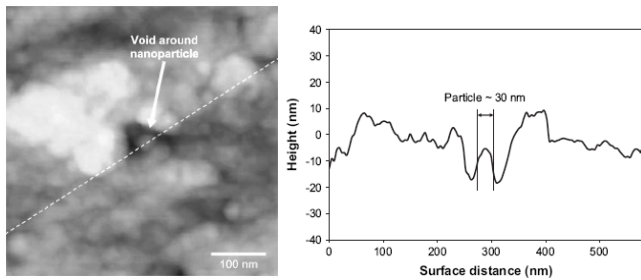


Fig. 4. Atomic force micrograph (height image) of a fracture surface of the epoxy polymer containing 9.6 vol% nanosilica as well as the surface profile of the line drawn across the nanosilica particle and void

4.3.2 Modelling of the contribution from the plastic void growth mechanism

To confirm whether the observed debonding and plastic void growth which occur for the nanoparticle-modified epoxy could be responsible for the toughening effect, the increase in toughness can be compared to a theoretical model. A suitable model for this is by Huang and Kinloch [12] where the contribution to the increase in fracture energy from the plastic void growth mechanism, ΔG_v , is given by:

$$\Delta G_v = (1 - \mu_m^2/3)(V_v - V_f)\sigma_{yc}r_{yu}K_{vm}^2$$

where μ_m mm is a material constant, V_v is the volume fraction of voids, V_f is the volume fraction of particles, σ_{yc} is the compressive yield stress of the unmodified epoxy polymer, r_{yu} is the radius of the plastic zone of the unmodified epoxy polymer, and K_{vm} is the maximum stress concentration factor of the von Mises stress in the plastic matrix. A comparison of the predicted and measured toughening increments is given in Table 2.

Table 2
Measured and predicted toughening increments

Nanosilica content (wt%)	Nanosilica content (vol%)	Toughening increment, Ψ (J/m ²)	
		Measured	Predicted
4.1	2.5	188	107
7.8	4.9	249	209
11.1	7.1	240	297
14.8	9.6	303	394
20.2	13.4	358	540

4.4 Conclusions

An epoxy resin cured with an anhydride has been used. This was modified by the addition of silica nanoparticles, manufactured using a sol-gel process, which were 20 nm in diameter. These particles were well-dispersed through the epoxy matrix with no agglomeration observed using transmission electron and atomic force microscopies. The addition of the nanoparticles did not affect the glass transition temperature; the T_{gs} of the unmodified and nanoparticle-modified epoxy polymers were measured to be in the range of 140±4°C using differential scanning calorimetry. Dynamic mechanical thermal analysis confirmed this observation. The addition of nanoparticles

increased the modulus of the epoxy polymer as expected. The fracture toughness of the polymers was measured, and a K_{Ic} of 0.59 MN m^{-3/2} was recorded for the unmodified epoxy. Addition of the nanoparticles increased the fracture toughness with a maximum value of 1.42 MN m^{-3/2} being measured for the epoxy polymer with 13.4 vol% of nanoparticles. These values were converted to fracture energies, G_{Ic} , using the measured modulus. The unmodified epoxy polymer gave $G_{Ic} = 103$ J/m², and a maximum fracture energy of 460 J/m² was calculated. Hence there is a significant toughening effect due to the addition of the silica nanoparticles. Observation of the fracture surfaces using scanning electron and atomic force microscopies showed nanoparticles surrounded by voids, providing evidence of debonding of the nanoparticles and subsequent plastic void growth. An analytical model of plastic void growth was used to confirm whether this mechanism could be responsible for the increased toughness. The mean void diameter was measured from the micrographs, and the model was used to predict the toughening increment (compared to the fracture energy of the unmodified epoxy polymer). The predicted values agreed well with the measured values, indicating that debonding of the nanoparticles and subsequent plastic void growth were most likely to be responsible for the increase in toughness that was observed due to the presence of the nanosilica particles.

4.5 References

- [1] Drake RS, Siebert AR. SAMPE Quart 1975;6(4):11e21.
- [2] Pascault JP, Williams RJJ. Formulation and characterization of thermoset-thermoplastic blends. In: Paul DR, Bucknall CB, editors. Polymer blends volume 1: formulation. New York, USA: John Wiley & Sons; 1999. p. 379-415.
- [3] Young RJ, Beaumont PWR. J Mater Sci 1975;10:1343e50.
- [4] Kinloch AJ, Taylor AC, Lee JH, Sprenger S, Eger C, Egan D. J Adhes 2003;79(8-9):867-73.
- [5] Sprenger S, Eger C, Kinloch AJ, Taylor AC, Lee JH, Egan D. Adhesion Kleben Dichten 2003;2003(3):24-8.
- [6] ISO-527-1. Plastics e determination of tensile properties - part 1: general principles. Geneva: ISO; 1993.
- [7] ISO-527-2. Plastics e determination of tensile properties - part 2: test conditions for moulding and extrusion plastics. Geneva: ISO; 1996.
- [8] ISO-13586. Plastics e determination of fracture toughness (G_{Ic} and K_{Ic}) - linear elastic fracture mechanics (LEFM) approach. Geneva: ISO; 2000.
- [9] Kinloch AJ, Taylor AC. J Mater Sci 2006;41(11):3271-97.
- [10] Kinloch AJ, Taylor AC. J Mater Sci 2002;37(3):433-60.
- [11] Andrews EH. Fracture in polymers. 1st ed. Edinburgh: Oliver & Boyd; 1968.
- [12] Huang Y, Kinloch AJ. J Mater Sci 1992;27(10):2763e9.
- [13] Johnsen, B.B., Kinloch A.J., Mohammed R.D., Taylor A.C., Sprenger S., Polymer 2007;48:530-541.